



Lawrence Berkeley Laboratory

UNIVERSITY OF CALIFORNIA

Submitted to Journal of Luminescence

Scintillation Mechanisms in Cerium Fluoride

W.W. Moses, S.E. Derenzo, M.J. Weber, F. Cerrina,
and A. Ray-Chaudhuri

February 1993

Donner Laboratory

Biology & Medicine Division

1 LOAN COPY 1
1 Circulates 1
for 4 weeks 1 Bldg. 50-Library.

LBL-27609

Copy 2

DISCLAIMER

This document was prepared as an account of work sponsored by the United States Government. While this document is believed to contain correct information, neither the United States Government nor any agency thereof, nor the Regents of the University of California, nor any of their employees, makes any warranty, express or implied, or assumes any legal responsibility for the accuracy, completeness, or usefulness of any information, apparatus, product, or process disclosed, or represents that its use would not infringe privately owned rights. Reference herein to any specific commercial product, process, or service by its trade name, trademark, manufacturer, or otherwise, does not necessarily constitute or imply its endorsement, recommendation, or favoring by the United States Government or any agency thereof, or the Regents of the University of California. The views and opinions of authors expressed herein do not necessarily state or reflect those of the United States Government or any agency thereof or the Regents of the University of California.

Scintillation Mechanisms in Cerium Fluoride

W.W. Moses and S.E. Derenzo

Life Sciences Division
Lawrence Berkeley Laboratory
University of California
Berkeley, CA 94720

M.J. Weber

Lawrence Livermore National Laboratory
University of California
Livermore, CA 94550

F. Cerrina and A. Ray-Chaudhuri

Synchrotron Radiation Center
University of Wisconsin
Stoughton, WI 53589

February 1993

This work was supported in part by the Director, Office of Energy Research, Office of Health and Environmental Research, of the U.S. Department of Energy under Contract No. DE-AC03-76SF00098, by Public Health Service under Grant Numbers P01 HL25840 and R01 CA38086 awarded by the National Heart, Lung and Blood and National Cancer Institutes, Department of Health and Human Services, by the U.S. Department of Energy, Division of Materials Sciences and Division of Chemical Sciences under Contract No. DE-AC02-76CH00016, by the NSF under Award No. DMR-9212658, by the U.S. Department of Energy under Contract No. W-7405-ENG-48, and by the Whitaker Foundation.

Scintillation Mechanisms in Cerium Fluoride

W.W. Moses and S.E. Derenzo,
Lawrence Berkeley Laboratory, 1 Cyclotron Rd., Berkeley, California 94720

and

M.J. Weber,
Lawrence Livermore National Laboratory, Livermore, California 94550

and

F. Cerrina and A. Ray-Chaudhuri,
Synchrotron Radiation Center, University of Wisconsin, Stoughton, Wisconsin 53589

Abstract

Ultraviolet photoelectron spectroscopy, optical transmission, fluorescence excitation spectroscopy, and time-resolved fluorescence spectroscopy are used to investigate the scintillation mechanisms of cerium fluoride (CeF_3) and of lanthanum fluoride doped with cerium in concentrations between 0.01% and 50% mole fraction cerium. In $\text{LaF}_3:\text{Ce}$ the absorption of either optical or ionizing radiation directly or indirectly results in excitation of the Ce^{3+} 4f electron to the lowest 5d level followed by 5d \rightarrow 4f fluorescence at 284–300 nm. Whereas for optical excitation the fluorescence has a 20 ns decay time, for ionizing radiation there is an additional faster (2–10 ns) initial decay component. As the cerium concentration increases, an another band appears that partially absorbs the 284–300 nm emission and re-radiates it in a broad band peaking at 340 nm and having a longer (~30 ns) decay time. In the limit of 100% CeF_3 , radiation trapping is very pronounced. The additional absorption and emission bands present at large Ce concentrations are attributed to Ce^{3+} ions in perturbed sites. The relative efficiency for excitation of unperturbed and perturbed cerium sites via the Ce^{3+} 5d and 6s bands, the F^- 2p valence band, and the Ce^{3+} or La^{3+} 5p core levels are determined from fluorescence excitation spectra.

Introduction

This paper investigates the mechanisms responsible for the scintillation of cerium fluoride (CeF_3) and cerium-doped lanthanum fluoride ($\text{LaF}_3:\text{Ce}$), a recently discovered family of high density scintillators of interest for gamma ray detection in both medical imaging and high energy physics applications [1, 2, 3, 4]. The observed scintillation spectra and decay kinetics of these materials are not simple and depend upon the particular crystals and experimental conditions used. Interest in understanding and improving the scintillation properties of CeF_3 is currently quite high, for at least one high energy physics collaboration is proposing to build an electromagnetic calorimeter containing as much as 60 cubic meters of CeF_3 [5, 6, 7]. The motivation for this study is a better understanding of the fluorescence mechanism with the objective of improving the scintillation light yield and decay time.

The photoluminescence of $\text{La}_{1-x}\text{Ce}_x\text{F}_3$, where $0 < x \leq 1$, has been studied by many investigators over the past 50 years [6, 8, 9, 10, 11, 12]. The free-ion $4f^1$ electronic ground state of Ce^{3+} is split by the spin-orbit interaction into two states $^2F_{5/2}$ and $^2F_{7/2}$ separated by 0.3 eV, and the excited 5d band is located 6.2 eV above the bottom of the 4f band [13]. When Ce^{3+} is introduced into LaF_3 , the crystal field depresses the 5d band by 1.3 eV (nephelauxetic shift) and splits it into five Stark components with an overall splitting of approximately 1.2 eV [10, 11]. Ions excited into the 5d or higher lying states of Ce^{3+} rapidly decay to the lowest 5d level from which fluorescence is observed to the two spin-orbit states of the 4f ground state [8, 9, 10, 14]. The observed Stokes shift of the 4f-5d transition is approximately 0.6 eV [9, 10, 14].

For cerium concentrations of several percent or more, additional longer wavelength fluorescence bands extending to at least 450 nm are observed [8, 9], and have been ascribed to cerium ions in sites perturbed by nearby defects [12]. The 284-300 nm emission is excited by wavelengths < 260 nm, whereas the longer wavelength emission is excited by wavelengths in the 260-310 nm region [8, 11].

The scintillation properties of CeF_3 have also been studied extensively and significant sample-to-sample variations are observed, particularly in the emission spectra and decay behavior [1, 2, 3, 4, 6, 12]. Radiation trapping effects are pronounced for materials having large cerium concentrations. Because of this, the emission spectrum of CeF_3 depends on the excitation source and the excitation-observation geometry used, so almost no two fluorescence spectra reported in the literature look the same. To cite an extreme example, Figure 1 shows the spectrum of a single crystal of CeF_3 excited with 511 keV gamma rays, which results in peaks at 310 and 340 nm, as well as the 20 keV x-ray excited spectrum of powdered CeF_3 , which is dominated by a single peak at 300 nm.

The decay of the 284-300 nm fluorescence of $\text{La}_{1-x}\text{Ce}_x\text{F}_3$ following pulsed optical excitation exhibits a simple exponential time dependence with a lifetime of approximately 20 ns at room temperature for both small and large values of x [9, 11, 14, 15]. The decay following excitation by ionizing radiation is different, however. While there is some disagreement between different groups as to the exact mathematical model that describes the data, there is a consensus that following a very fast rise time (< 1 ns), there is a multi-exponential decay dominated by a 27-30 ns component [1, 2, 3, 4, 12]. An additional fast decay component is observed after excitation by ionizing radiation (values between 2 and 10 ns are quoted) — similar fast components have been reported for Ce^{3+} in several other crystals and glasses excited by ionizing radiation [16, 17, 18]. Finally, a weak, very long (several hundred ns) scintillation component has also been reported [3]. Neither the fast nor slow component has been observed in the $\text{La}_{1-x}\text{Ce}_x\text{F}_3$ system or in these other cerium doped materials when optically excited.

The long (340-450 nm) wavelength emission observed for large x values, in addition to extending over a wide wavelength range, exhibits a variation of decay time with wavelength [11], which is evidence for the existence of several physically different, perturbed Ce^{3+} sites. After excitation by either non-selective pulsed optical radiation or ionizing radiation, the longer

wavelength emission exhibits both prompt and slower rise time components due to a combination of direct excitation of perturbed sites and excitation by energy transfer from unperturbed Ce^{3+} sites. A typical set of fluorescence time dependencies observed for excitation by ionizing radiation are shown in Figure 2 (exerpted from [3]).

The $\text{La}_{1-x}\text{Ce}_x\text{F}_3$ system, where $0 < x \leq 1$, is an ideal system for studying the Ce^{3+} fluorescence because the interactions between optically active Ce^{3+} ions can be reduced by replacing them with La^{3+} ions which have very similar physical and chemical properties but are optically inactive. In this family of compounds the cerium luminescence is not strongly concentration quenched. Below we have used several different spectroscopies—ultraviolet photoelectron spectroscopy, optical absorption and emission spectra, and fluorescence excitation spectra—to probe the scintillation mechanisms in CeF_3 .

Experimental Methods

Six crystalline samples provided by Optovac, Inc. were studied: undoped CeF_3 , cerium doped into LaF_3 in four concentrations (50%, 10%, 1%, and 0.01% mole fraction cerium), and undoped LaF_3 . Crystal sample orientations were not known, nor were the polarization properties of any of the excitation beams. The samples were not analyzed to determine exact dopant or impurity concentrations. Similar samples manufactured by the same source have been found to have rare earth impurities at the level of a few hundred parts per million level [12], typically neodymium and praseodymium. All measurements were made with the samples at room temperature.

We have used two vacuum ultraviolet synchrotron radiation techniques and one optical technique to investigate the samples. Ultraviolet photoelectron spectroscopy (UPS) [19] was used to determine the energies of the populated electron energy bands of the compounds. A freshly cleaved crystalline sample was irradiated with monochromatic 50 eV photons from the Aluminum Seya-Namioka beamline at the Synchrotron Radiation Center (SRC) at the University of Wisconsin. This beam photoionized the sample and the kinetic energy spectrum of the emitted photoelectrons was recorded with 0.1 eV resolution using a commercial cylindrical mirror electron energy analyzer.

Fluorescence spectra were measured by exciting the surface of a freshly cleaved crystal with monochromatic 20 eV photons. The resulting front-surface fluorescence was analyzed with a 0.125 m grating monochromator blazed at 300 nm and detected with a cooled, quartz windowed photomultiplier tube (PMT). These spectra were corrected for spectral variations in the photomultiplier tube and monochromator efficiency using a calibrated deuterium light source.

Fluorescence excitation spectra were recorded by irradiating the sample with monochromatic ultraviolet photons from the SRC [20, 21, 22]. The intensity of a given emission line was monitored by the above analyzing monochromator and photomultiplier tube as the excitation beam energy was scanned. For excitation energies below 8 eV, a sapphire window was placed between the incident beam and the sample to remove the effects of excitation by higher order light passed by the beamline monochromator. Reported spectra were corrected to give constant incident beam intensity (photons / second) using a calibration curve derived from measurements made with a GaAsP photodiode.

Optical transmission spectra of 3 mm thick polished samples were measured using a commercial split-beam spectrophotometer with deuterium and tungsten light sources and a quartz windowed photomultiplier tube.

Results

Ultraviolet Photoelectron Spectroscopy

Ultraviolet photoelectron spectra of $\text{La}_{1-x}\text{Ce}_x\text{F}_3$ are shown in Figure 3 for $x = 0, 0.0001, 0.01, 0.1, 0.5$ and 1.0 . The electron binding energy is the difference between the incident photon energy and the emitted photoelectron kinetic energy, therefore the electron population density as a function of binding energy can be determined from this data. The exact position of the peaks have an approximately 1 eV uncertainty due to electrostatic charging of the sample, which we attempted to minimize by flooding the surface of the crystals with thermal electrons. Peaks corresponding to electron energy bands are evident in these plots at 12 eV and 8 eV binding energy. The area under the peak at 8 eV decreases roughly proportionally to cerium fraction and is identified as the Ce^{3+} 4f peak. The peak at 12 eV has 16.5 times the area of the Ce^{3+} 4f peak. Since there are 18 F^- 2p electrons for each Ce^{3+} 4f electron in CeF_3 , this larger peak is assigned to the F^- 2p valence band. Weak peaks are also observed for CeF_3 at about 24 and 27 eV which are a reasonable expectation for the 5p core levels of Ce. The binding energies of the F 2s and the Ce 5s levels are expected to be in the region of 30 to 40 eV, and so not observed in these data. The widths and spacing of the peaks in our spectra agree with earlier measurements in CeF_3 [23], however there is a large (4 eV) shift in the absolute value of the binding energy.

Optical Transmission

Optical transmission spectra for CeF_3 and $\text{LaF}_3:\text{Ce}$ are shown in Figure 4. The 4f \rightarrow 5d absorption bands in the 0.01% cerium sample are observed at 254, 240, 223, 210, and 195 nm, in good agreement with previous measurements [9, 10, 11]. These absorption bands are located at 4.9, 5.2, 5.6, 5.9, and 6.4 eV above the 4f ground state (which the UPS measurement locate at 8 eV binding energy), implying that the 5d bands have binding energies of approximately 3.1, 2.8, 2.4, 2.1, and 1.6 eV. For Ce concentrations of $\geq 1\%$ and the sample thicknesses used, the absorption by the 4f-5d transitions becomes so strong that there is over-absorption and the individual levels are no longer resolved. A single cutoff edge is observed whose position ranges from 275 nm in the 1% cerium sample to 300 nm in the CeF_3 sample. The 50% cerium sample shows a decrease in transmission between 300 and 400 nm similar to that observed in CeF_3 samples that are contaminated by oxygen [7].

Fluorescence Spectra

Fluorescence spectra of the six samples excited with 20 eV photons are shown in Figure 5. Because of the strong absorption of 20 eV photons, the emission is due predominantly from near surface Ce ions. The spectra as shown are corrected for spectral variations in the detection monochromator and photomultiplier tube efficiency, and have a spectral resolution of 12 nm. Additional emission spectra were taken with excitation energies between 4.3 and 27 eV in 2 eV increments; no additional significant emission lines were noted.

All samples have prominent peaks centered at 284 nm and 300 nm which are attributed to transitions from the lowest 5d level to the $^2\text{F}_{5/2}$ and $^2\text{F}_{7/2}$ levels of the 4f ground state. The wavelengths, widths, and relative intensity of these two peaks agree with the previous measurements of the optically excited fluorescence spectra of Ce-doped LaF_3 . Samples with $\geq 10\%$ cerium concentration have an additional broad emission band extending to almost 500 nm with a peak centered at approximately 340 nm. As shown in Figure 1, the 340 nm peak can, depending on the observation scheme, dominate the gamma-excited emission spectrum of CeF_3 and $\text{LaF}_3:\text{Ce}$ [8, 9, 10, 14].

The samples with $\leq 1\%$ cerium also have a weak, broadband luminescence extending from 250 to 500 nm and well defined peaks at approximately 395 and 480 nm. The broadband emission is attributed to radiative decay of self-trapped excitons (STE). Similar emission has been observed in LaF_3 doped with low ($\ll 1$ mole %) concentrations of Nd^{3+} [24]. The weak

peak at 395 nm and the pronounced peak 480 nm are attributed to Pr^{3+} impurities, as discussed later.

Fluorescence Excitation Spectra

The $5d \rightarrow 4f$ emission results in two lines at 284 and 300 nm that originate from the same lowest 5d level. As expected, there is no difference in the excitation spectrum for these two lines, so we collected data at an intermediate wavelength of 290 nm. The excitation spectra of the $5d \rightarrow 4f$ emission at 290 nm, corrected to give constant incident beam intensity, are shown in Figure 6. Strong peaks are observed between 4.5 eV and 6.5 eV excitation energy. The 0.01% cerium sample shows that there are five peaks located at 5.0, 5.3, 5.7, 6.0, and 6.5 eV in agreement with the observed absorption maxima in the transmission spectra. These peaks increase in intensity and merge into an unresolved band with increasing cerium concentration. There is an additional peak at 8.5 eV in the 0.01% cerium sample that is attributed to promotion from the 4f level to the 6s level, followed by relaxation to the lowest 5d level and a subsequent $5d \rightarrow 4f$ transition [11]. This line also increases in strength and merges into the levels of the 5d state with increasing cerium concentration.

The excitation spectra of all samples in Figure 6 show a sharp increase at 10–11 eV. The lower binding energy edge of the F^- 2p band from the UPS data in Figure 3, the UPS data in reference [23], and the reflectivity spectra in reference [25] are of comparable energy, thus we assign this increase to an atomic-like F^- 2p \rightarrow 3s transition and possibly F^- 2p to Ce^{3+} 5d interband transitions. In the first case, fluorescence follows from hole transfer to the Ce^{3+} , electron migration to the Ce^{3+} 5d band, and finally $5d \rightarrow 4f$ emission. As the excitation energy increases, the photoionized electron has sufficient kinetic energy to travel far enough from the point of ionization that it is not captured by a nearby cerium and the probability of luminescence decreases. There is a weak band at about 17 eV which may be due to excitation from valence band states to higher lying regions of the conduction band. Interband F^- 2p to Ce^{3+} 5d, 6s transitions would lead to the formation of Ce^{2+} with a 4f5d ground state, however, we have no direct evidence of this. Finally, there is a broad band centered near 22 eV that corresponds to a similar feature observed in the UPS data and is attributed to the Ce^{3+} 5p \rightarrow 5d, 6s and conduction band transitions. The spin orbit splitting of the 5p_{1/2} and 5p_{3/2} states of roughly 3 eV observed in UPS and reflectivity spectra [23, 25] is not resolved in our excitation spectra.

The fluorescence excitation spectrum of the 340 nm emission is shown in Figure 7. It is qualitatively very similar to that of the 290 nm emission with intense peaks observed between 4.5 and 6.5 eV, a narrow peak at 10–11 eV, and a broad band centered at 22 eV. There is an additional strong excitation peak at 4.4 eV for all samples with $\geq 1\%$ cerium; the relative strength of this peak increases with increasing cerium concentration. This agrees with previous measurements of CeF_3 excitation spectra made at room temperature and at 10 K [11], which showed an intense broad band extending from 4.4 to 5.0 eV.

The fluorescence excitation spectra of the 395 and 480 nm emissions, plotted in Figures 8 and 9, are generally quite weak and have spurious peaks at 6 and 5 eV, respectively, due to incident excitation light being observed in second order in the analyzing monochromator. There is a sharp increase between 6.4 and 8.5 eV in the low ($\leq 1\%$) cerium concentration samples — similar quality data from the 10% and 50% cerium samples is not available, but no large structures were seen in this range. The shape of this excitation spectrum is very similar to that of Pr^{3+} -doped LaF_3 [26]. Since praseodymium-doped LaF_3 fluoresces at 395 and 480 nm (the $^1\text{S}_0 \rightarrow ^1\text{I}_6$ and $^3\text{P}_0 \rightarrow ^3\text{H}_4$ transitions, respectively) [9], the structures between 6.4 and 8.5 eV are attributed to the 5d bands of praseodymium impurities. Nd^{3+} impurities in LaF_3 also have fluorescence lines in the vicinity of 395 nm, hence the 5d bands of Nd^{3+} impurities could also appear in the 395 nm excitation spectrum.

Because the STE luminescence of LaF_3 in Figure 5 extends from 250 to 500 nm, the 290, 340, 395, and 450 nm excitation spectra of the Ce-doped samples all contain features character-

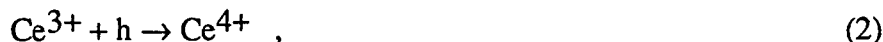
istic of the undoped LaF₃ sample. For the 0.01% cerium sample, this STE emission is nearly as large as the cerium emission at all excitation energies. For larger cerium concentrations the STE emission is much smaller than the cerium emission, except when the excitation energy is 10–12 eV. Since this excitation energy for strong STE emission corresponds closely to the position of the F⁻ 2p band, we feel that the STE is associated with the F⁻ site. This assumption is strengthened by the fact that the STE emission strength is nearly independent of cerium concentration, as well as the lack of a similar peak at 10–12 eV in the excitation spectrum of LaPO₄:Ce and other oxide hosts [21, 22].

Discussion

The dominant optical transition observed in all samples is the Ce³⁺ 5d–4f transition. As noted earlier, excitation spectra show that this fluorescence is caused by optical excitation of an electron from the 4f ground state to levels of the 5d and 6s states or by ionizing an electron from the F⁻ 2p valence band or deeper anion and cation core states. In the first case the excited (Ce³⁺)^{*} will emit a 5d→4f photon via



In the latter case, an F hole may be filled by a 4f electron from a nearby Ce³⁺. The resulting Ce⁴⁺ can then capture an electron and relax to the metastable 5d state followed by 5d→4f emission. That is,



and subsequent decay by the process in Equation (1). A hole created by photoionization of the Ce³⁺ 5p band can be filled by the 4f electron. The Ce⁴⁺ resulting from this intra-cerium process can then become excited by capture of an electron via Equation (3). In all cases, the electron capture may be either prompt arising from free electrons created in the initial absorption process, in which case the observed scintillation is limited by the (Ce³⁺)^{*} decay time, or delayed requiring the thermal activation of electrons from traps such as anion vacancies, in which case the delayed scintillation appears as an afterglow. The reported long (several hundred ns) decay component in the fluorescence decay of Ce-doped LaF₃ [3] suggests that such defects may also be present in some crystals.

Long Wavelength Emission

The samples with ≥10% cerium concentration can show significant emission at longer wavelengths. Reference [12] attributes the 340 nm emission to perturbed cerium ions and the data reported herein support that assumption. The intensity of the additional luminescence bands of CeF₃ relative to the normal 5d→4f fluorescence varies with starting materials and growth conditions, thus suggesting that it arises from Ce³⁺ sites perturbed by nearby impurities or defects. Trivalent lanthanide impurities such as La, Pr, Nd would substitute at Ce sites but would have only a small effect because of their similar size and valence state. Nearby substitutional or interstitial transition-metal impurities of various valence states could cause larger effects, however the presence of nearest-neighbor fluorine vacancies, interstitial fluorine, or substitutional oxygen would cause the largest effects. In a study of the concentration-dependent luminescence of Ce³⁺ in CaS, an additional longer wavelength emission was observed and attributed to the presence of oxygen [27]. Oxygen is undoubtedly present to some degree in all of the fluoride materials studied to date, however because of experimental difficulties, impurity concentrations have not been quantified. The more covalent bond of oxygen would shift the absorption and emission bands of CeF₃ to longer wavelengths and alter the decay rates, both of which are observed experimentally.

The long wavelength emission is excited by light in the 4.4–5.0 eV region which would correspond to the 5d states of perturbed Ce^{3+} sites. The expected five peaks are not observed in the excitation spectra, however. This is due in part because some of the levels may overlap the 5d peaks of the unperturbed sites and be masked. In addition, the bands may be inhomogeneously broadened. There are nine fluorine ions in the first coordination shell of cerium: two at 2.400, one at 2.419, two at 2.445, two at 2.460 and two at 2.621, plus two more at 2.974 Å [28]. Fluorine vacancies or anion impurities (such as oxygen) substituting for fluorines in the first coordination shell would affect the Ce^{3+} spectra. Because these defects can be located at several different distances from the cerium ions, the different local fields would result in inhomogeneously broadened spectra. As these effects would tend to increase the apparent splitting of the 5d states, it is curious that the width of the excitation spectrum for these perturbed cerium atoms (4.4–5.0 eV) is significantly less than that of the unperturbed atoms (5.0–6.5 eV).

Energy Transfer

Because the emission from regular Ce^{3+} sites overlaps the absorption band of perturbed Ce^{3+} site, light emitted in the CeF_3 system at ~290 nm is absorbed and subsequently re-emitted at 340 nm. This is confirmed by the strong correlation between the 290 and 340 nm fluorescence excitation spectra shown in Figures 6 and 7, and is further supported by the time-resolved fluorescence shown in Figure 2. The latter figure shows that the risetime of the 340 nm emission is roughly equal to the initial decay time of the 290 nm emission, which would be necessary for an energy transfer process. The transfer may be either radiative or nonradiative; the overlap between between emission and excitation bands allows a photon mediated transfer of energy.

To test this hypothesis, we compared the relative intensities of the 290 and 340 nm excitation spectra. Figure 10 plots the 340 nm intensity divided by the sum of the 340 and 290 nm intensities as a function of excitation energy. If the 340 nm excitation is caused solely by the absorption of 290 nm light, the ratio would be a constant (*i.e.* independent of excitation energy) and its magnitude would be a measure of the coupling strength. Any process that stimulates the 340 nm emission without stimulating the 290 nm emission will increase this ratio.

The relative fraction of 340 nm light in samples with $\geq 10\%$ cerium is significantly greater than it is in samples with 1% cerium and, with three notable exceptions, the fraction is independent of excitation energy. The first exception is that all samples show a strong increase in 340 nm emission at 4.4 eV arising from the shifted 5d excitation band of perturbed ions. The second exception is a strong increase near 10 eV in the four samples with $\geq 1\%$ cerium concentration, and is due to STE emission, which contributes to both the 290 and 340 nm emissions. Note that for the sample with 0.01% cerium, the STE emission dominates in all regions except 5.0 to 6.5 eV. The final exception occurs at excitation energies between 7 and 10 eV in the 100% CeF_3 sample and may be due to distortion caused by over absorption.

Quantum Efficiency

The excitation spectra in Figure 6 also provide information about the quantum efficiency, defined as the average number of emitted fluorescent photons per incident excitation photon. The radiative quantum efficiency of the Ce^{3+} 5d \rightarrow 4f emission is expected to be high based on the measured 20 ns lifetime, which is the order of magnitude of that expected from the oscillator strength, and the fact that the onset of thermal quenching by multi-phonon processes does not occur until 300–400 K [4, 15]. The fluorescence risetime following excitation into the higher lying 5d and 6s bands is very fast (< 1 ns), hence the overall quantum efficiency is still high. The energy efficiency, however, decreases because of the quantum defect, that is, the energy lost in the nonradiative decay from the initial excited state to the emitting state.

In contrast to these intra-cerium excitation and decay processes, activation of the Ce^{3+} 5d \rightarrow 4f fluorescence via absorption by F⁻ 2p or deeper core levels involves a transfer efficiency and several intervening processes and has a lower quantum efficiency. Inner shell excitation

followed by various secondary processes eventually leads to thermalized electrons and holes. These charge carriers may recombine radiatively or nonradiatively, be trapped or captured by cerium ions via the processes in Equations 2 and 3, or form excitons. The absorption coefficients of CeF_3 in the extreme ultraviolet are $10^{-5} - 10^{-6} \text{ cm}^{-1}$, so light is absorbed in a layer about 0.01–0.1 nm thick. The concentration of defects near the surface is greater than in the volume, and as these defects can act as centers for nonradiative recombination of electrons and holes, this can give rise to a changing quantum efficiency with wavelength and penetration depth.

In samples containing $\geq 1\%$ Ce, where the relative effects of impurities and STE luminescence are smaller, the amplitudes of the $\text{F}^- 2s$ and the $\text{Ce}^{3+} 5p$ peaks are an order of magnitude or more smaller than the $5d-6s$ excitation peaks. The $\text{Ce}^{3+} 5p$ peak increases relative to the $5d$ peak with increasing Ce concentration. This indicates that the photoelectron is not simply captured by the Ce ion from which it originated, but migrates to other, more distant Ce ions. The $\text{F}^- 2p$ peak also increases with increasing Ce concentration. This peak is also observed in excitation spectra of rare earths on LaF_3 at 10–13 eV but a prominent $\text{O}^{2-} 2p$ peak near 10 eV is not observed for rare earths in oxide hosts [21, 22].

For CeF_3 the $5p$ peak is less than one-half of that of the $5d$ bands. Since the excitation spectra as shown are for constant quantum efficiency (*i.e.* constant incident photon flux), the energy efficiency for $5p$ excitation is much less than unity. The results of quantum efficiency measurements for cerium dopants in other oxide and fluoride host are mixed. For $\text{YPO}_4:\text{Ce}$ the relative quantum efficiency in the 12–22 eV region is comparable to that of the $5d$ bands; for Tb^{3+} , however, it is only ~ 0.3 at 20 eV [29]. The former result is puzzling, whereas the latter result is in qualitative agreement with the measured quantum efficiency for Ce^{3+} in LaPO_4 near 22 eV [22]. The absolute quantum efficiency for $\text{LaPO}_4:\text{Ce}$ is ~ 0.15 at 25 eV (see Figure 9 of Ref. [22]). Absorption by deeper core levels will, via Auger and other processes, lead eventually to multi-photon emission [22] and, at a sufficiently high energy, an approximate linear dependence on input energy (except for regions of characteristic absorption edges). The light yield of CeF_3 for ionizing radiation is only 10% that of $\text{NaI}(\text{Tl})$ [1, 2, 3, 4, 6] and the energy efficiency of the latter is only 11% [30]. Therefore the radiative quantum efficiency of CeF_3 for ionizing radiation will become greater than unity only for input energies greater than several hundred eV.

To determine the energy dependence of the CeF_3 quantum efficiency, we extended the fluorescence excitation spectrum for the 290 and 340 nm emission lines of CeF_3 to excitation energies up to 200 eV using the Vanderbilt 6-meter Toroidal Grating Monochromator beamline at SRC. These data, shown in Figure 11, are corrected to constant incident beam intensity using a beamline calibration derived from a gold diode. The quantum efficiency of the 290 nm line was normalized to 0.15 at 25 eV — the same as $\text{LaPO}_4:\text{Ce}$ [22]. A similar value is obtained if the excitation spectrum is normalized using a $5d$ band quantum efficiency of near unity. The relative quantum efficiency of the 340 nm emission is also included for comparison, but its apparent quantum efficiency depends on experimental conditions. The quantum efficiency increases nearly linearly for energies above 70 eV, except for a dip at 120 eV that is due to the $\text{Ce}^{3+} 4d$ excitation. As anticipated based on the reported relative light yield, the quantum efficiency is less than unity even at 200 eV, but if the curve is extrapolated to higher energies, would reach unity at approximately 250 eV.

Conclusion

We have studied the surface-excited fluorescence from CeF_3 doped into LaF_3 at a variety of concentrations. The dominant emissions are at 284 nm and 300 nm due to allowed $5d \rightarrow 4f$ transitions of Ce^{3+} . These emissions are partially absorbed by cerium ions that have been perturbed in some way, either by impurities, crystal defects, or interactions with other cerium ions. These perturbed ions emit fluorescence in a broad band peaking at 340 nm with about a 30 ns decay time constant. Because the 340 nm light is emitted with a slower decay time than the 290 nm light, this absorption and re-emission increases the effective decay time, which degrades

the performance of CeF_3 as a scintillator. The data imply that the scintillation properties of CeF_3 can be improved if perturbed sites can be eliminated. This may be possible if the perturbation is caused by an impurity or introduced in the manufacturing process, but would not be impossible if it is due to cerium-cerium interactions.

For excitation with ionizing radiation there is an initial fast (2–10 ns) decay time component. This can arise from ions that have an enhanced radiative or nonradiative decay probability. If the faster decay is due to non-radiative quenching, it would reduce the radiative quantum efficiency. The cause and mechanism for the fast decay remains unresolved.

Acknowledgments

We would like to thank Robert Sparrow of Optovac, Inc. for providing the CeF_3 crystals used in this work and Dr. Charles Bouldin of the National Bureau of Standards for use of Beam Line X23A2 at NSLS, as well as Dr. Alexander Lempicki, Dr. Andy Wojtowicz, and Dr. Edward Berman of Boston College for many useful discussions. This work was supported in part by the Director, Office of Energy Research, Office of Health and Environmental Research of the U.S. Department of Energy, under contract No. DE-AC03-76SF00098, and in part by Public Health Service Grant Numbers P01 HL25840 and R01 CA38086 awarded by the National Heart Lung and Blood and National Cancer Institutes, Department of Health and Human Services. Research carried out in part at the National Synchrotron Light Source, Brookhaven National Laboratory, which is supported by the U.S. Department of Energy, Division of Materials Sciences and Division of Chemical Sciences under contract No. DE-AC02-76CH00016. A portion of this work is based on research conducted at the Synchrotron Radiation Center, University of Wisconsin, which is supported by the NSF under Award No. DMR-9212658. The work of MJW was performed under the auspices of the U.S. Department of Energy by the Lawrence Livermore National Laboratory under Contract No. W-7405-ENG-48. WWM gratefully acknowledges The Whitaker Foundation for support.

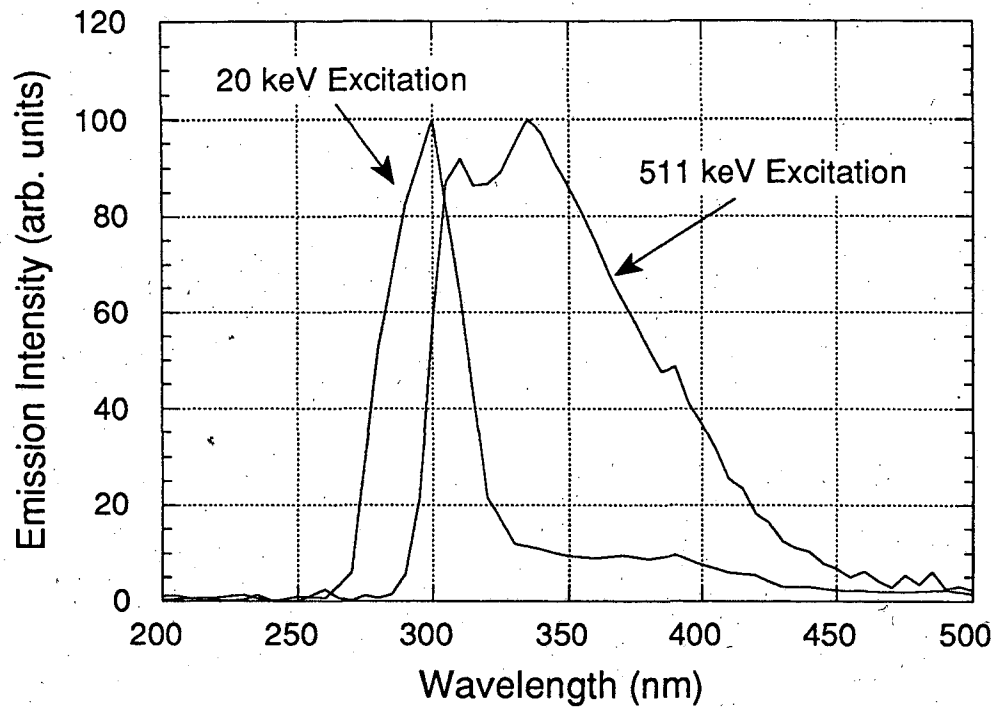


Figure 1: Emission spectra (independently normalized to 100) for powdered CeF₃ excited by 20 keV x-ray photons and crystalline CeF₃ excited by 511 keV gamma rays.

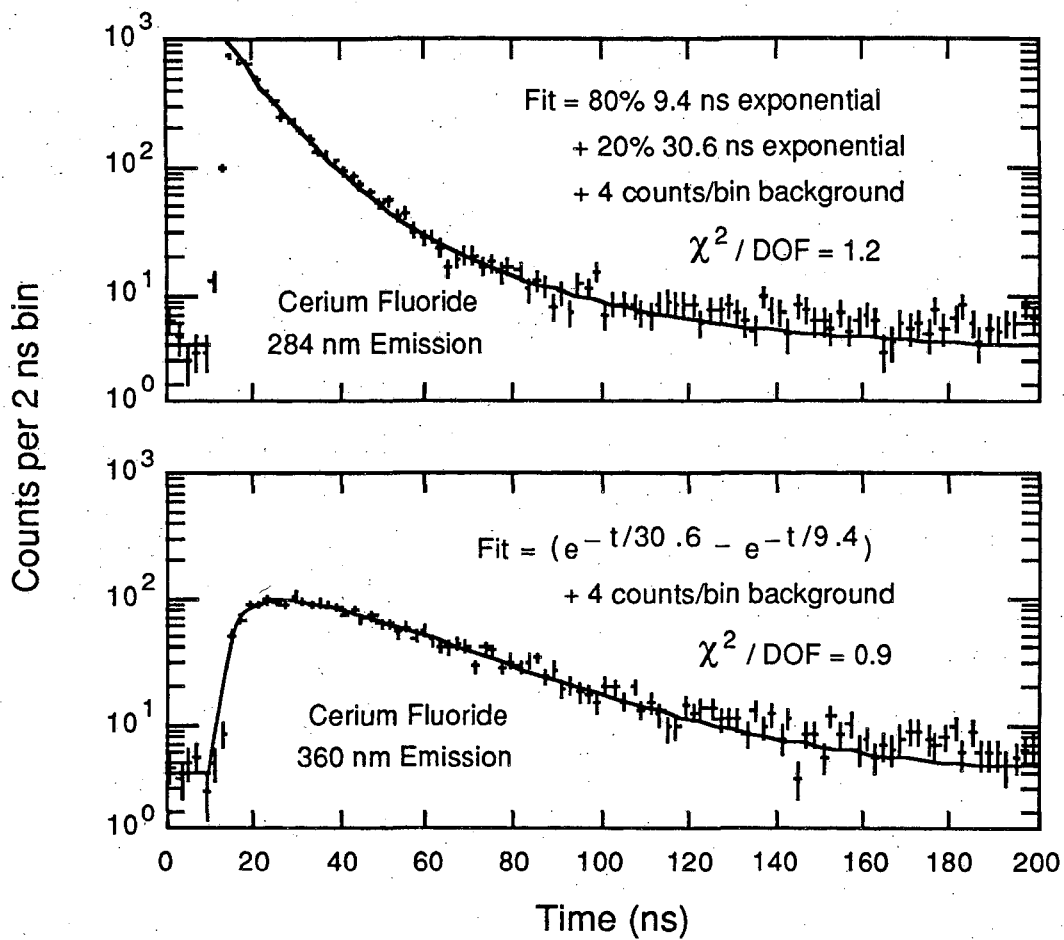


Figure 2: Time resolved spectra for CeF₃ excited by 20 keV x-rays.

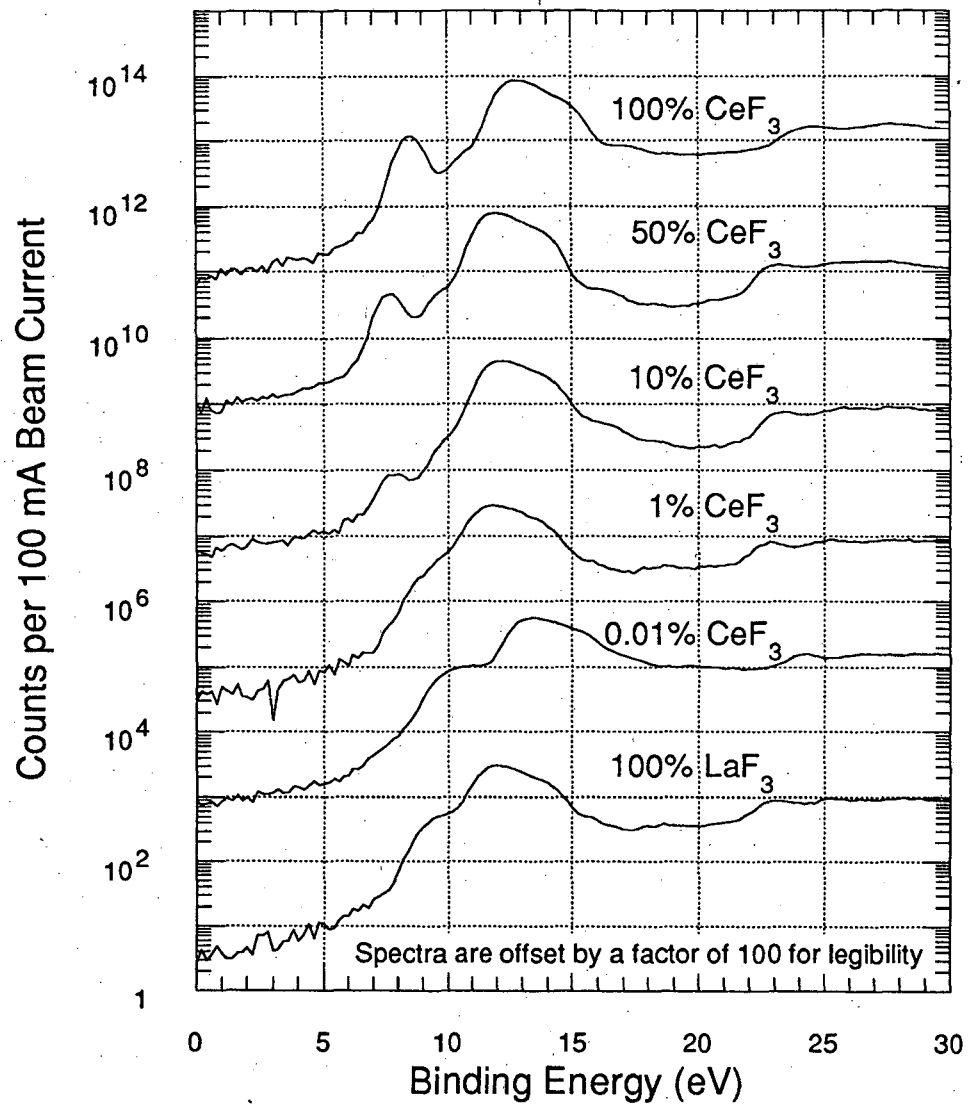


Figure 3: Ultraviolet photoelectron emission spectra for CeF_3 , $\text{LaF}_3:\text{Ce}$, and LaF_3 .

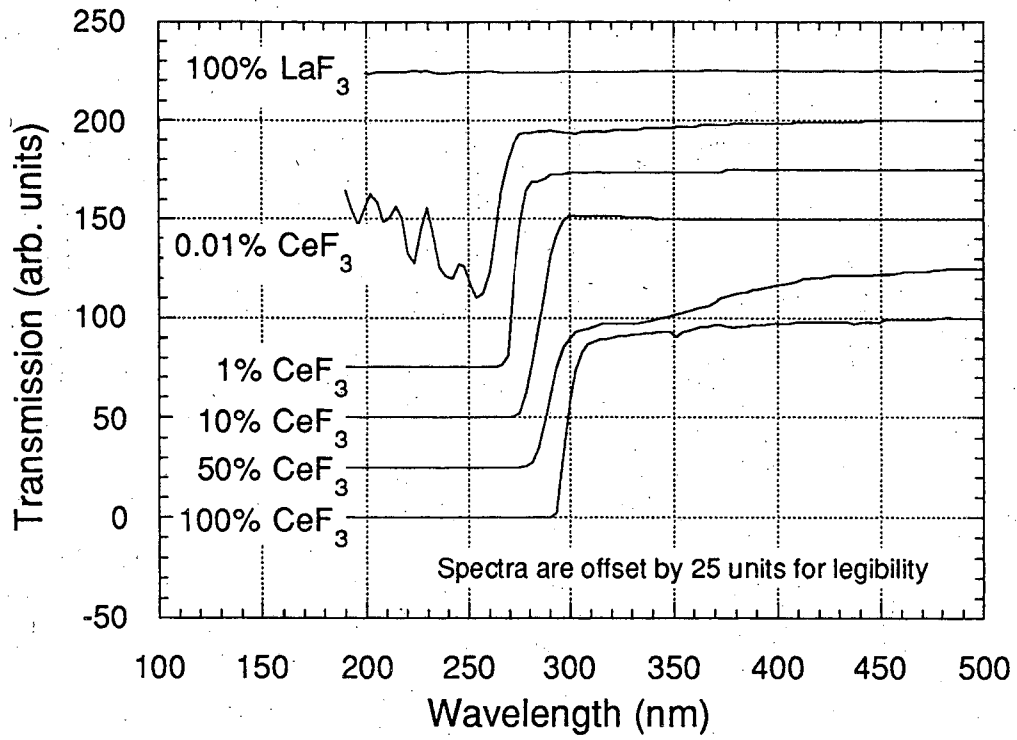


Figure 4: Transmission spectra for CeF_3 and $\text{LaF}_3:\text{Ce}$.

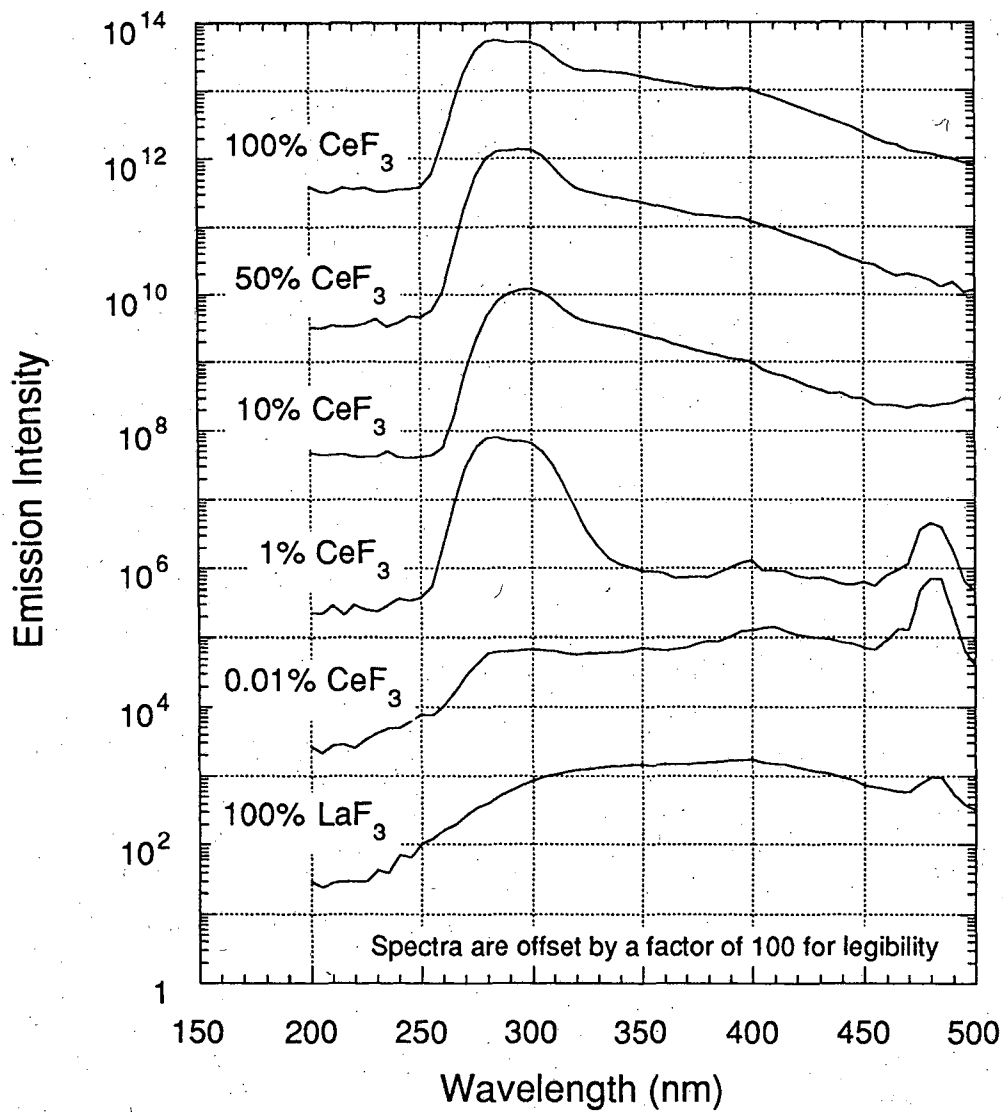


Figure 5: Surface emission spectra for CeF_3 , $\text{LaF}_3:\text{Ce}$ and LaF_3 excited with 20 eV photons.

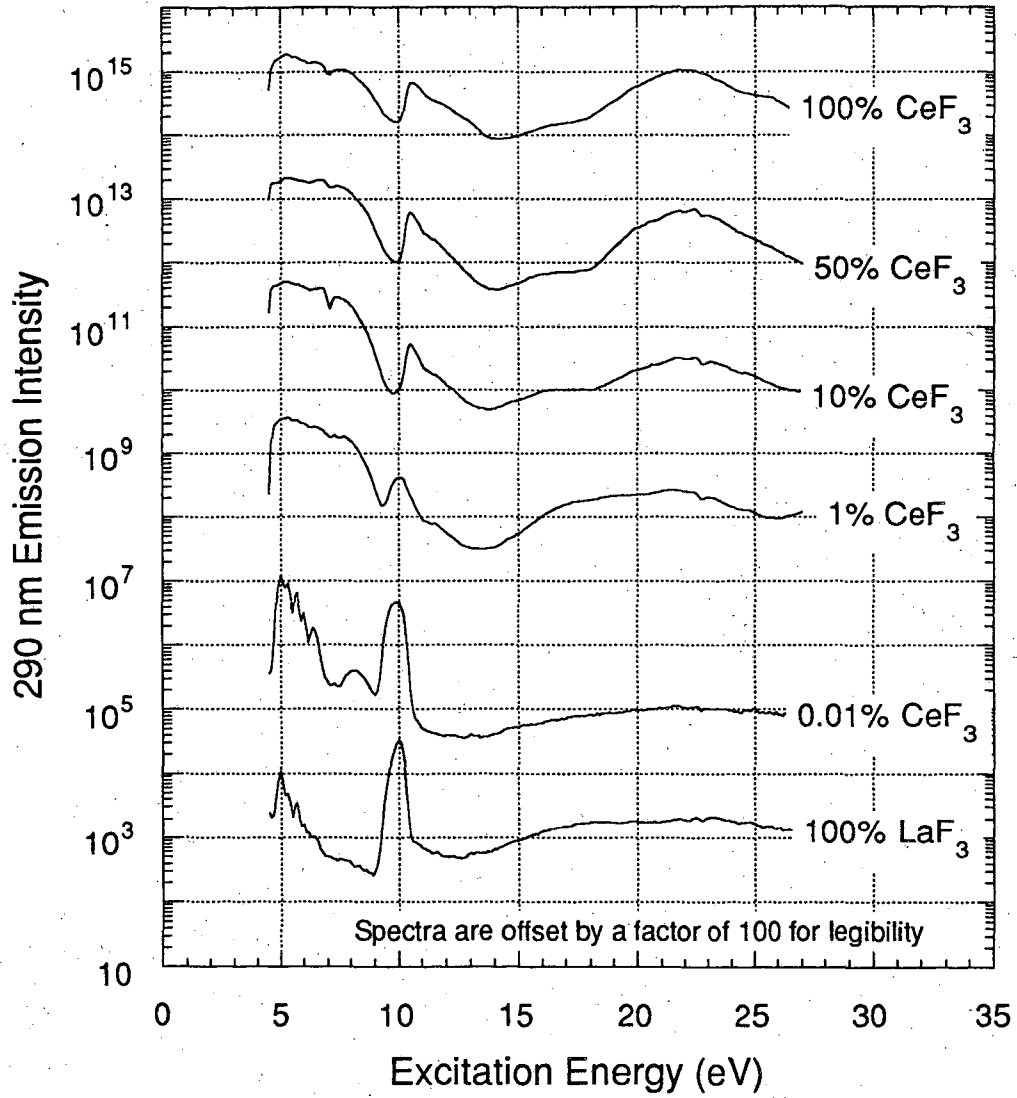


Figure 6: Fluorescence excitation spectra of the 290 nm emissions in CeF₃, LaF₃:Ce and LaF₃.

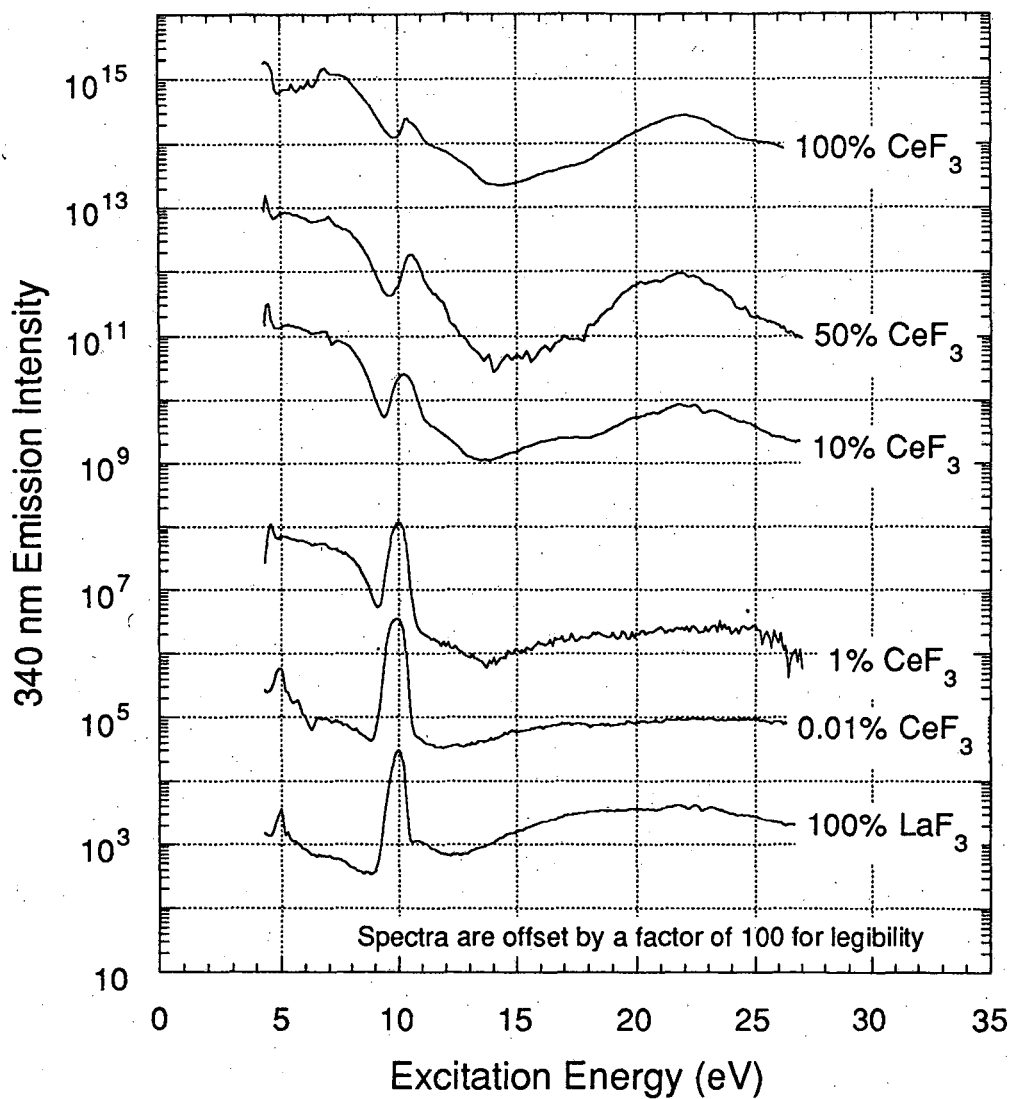


Figure 7: Fluorescence excitation spectra of the 340 nm emissions in CeF₃, LaF₃:Ce and LaF₃.

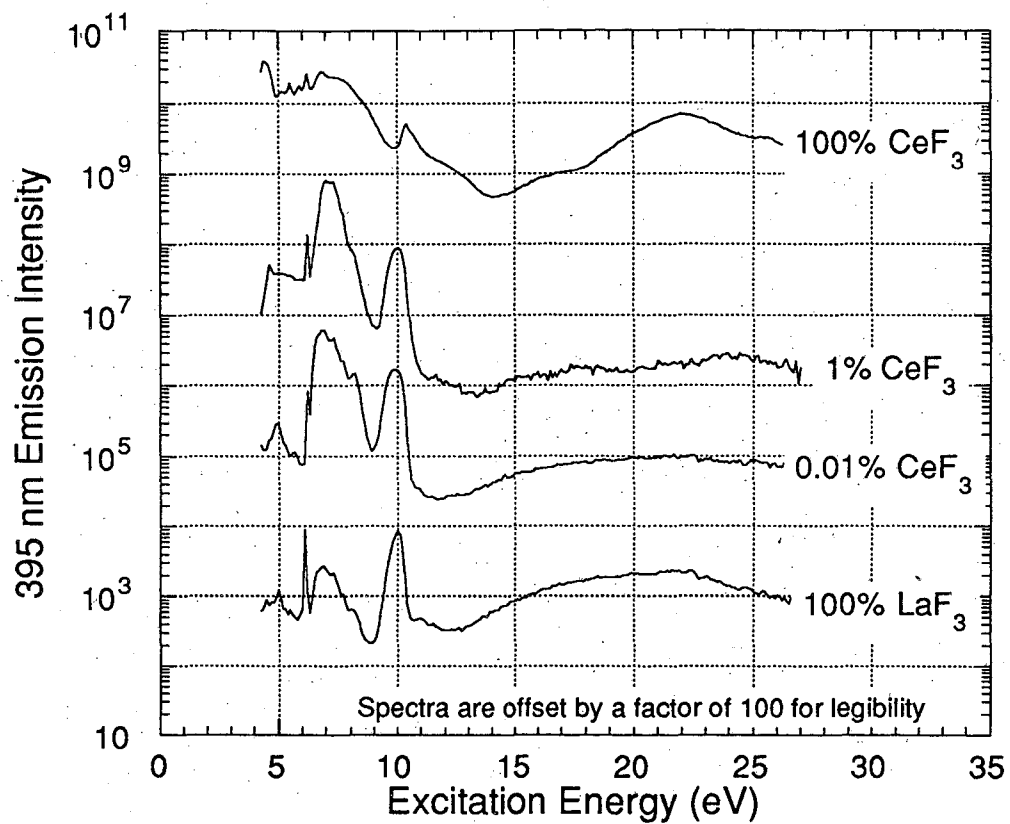


Figure 8: Fluorescence excitation spectra of the 395 nm emissions in CeF_3 , $\text{LaF}_3:\text{Ce}$ and LaF_3 .

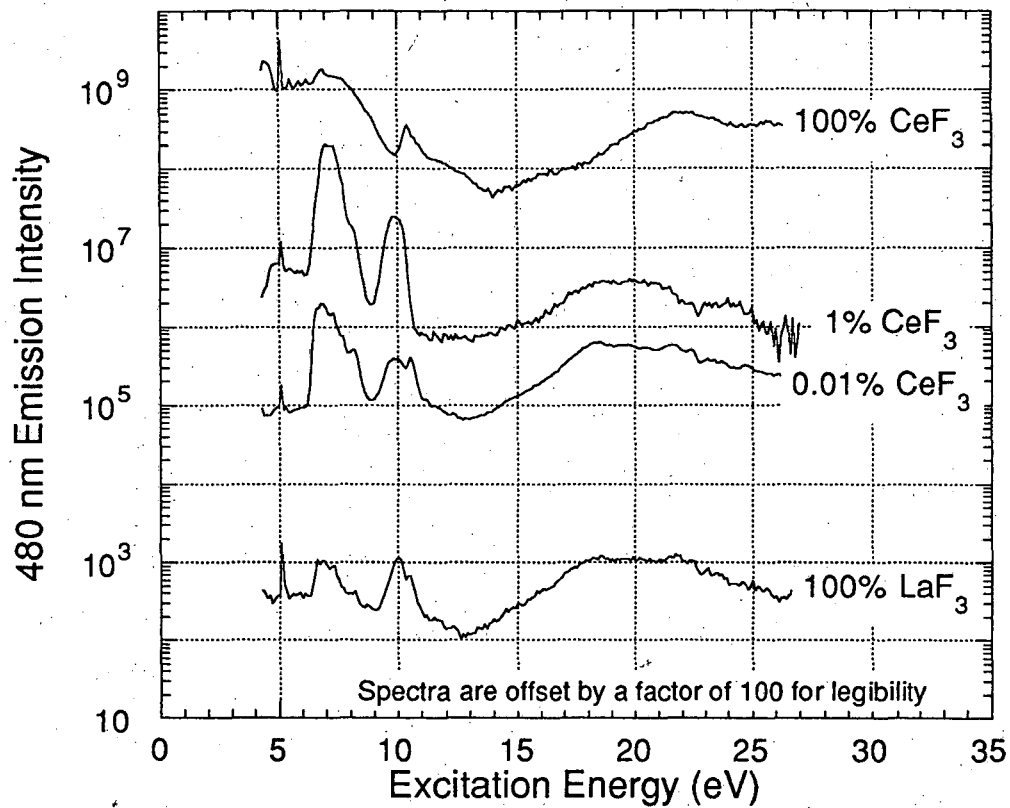


Figure 9: Fluorescence excitation spectra of the 480 nm emissions in CeF_3 , $\text{LaF}_3:\text{Ce}$ and LaF_3 .

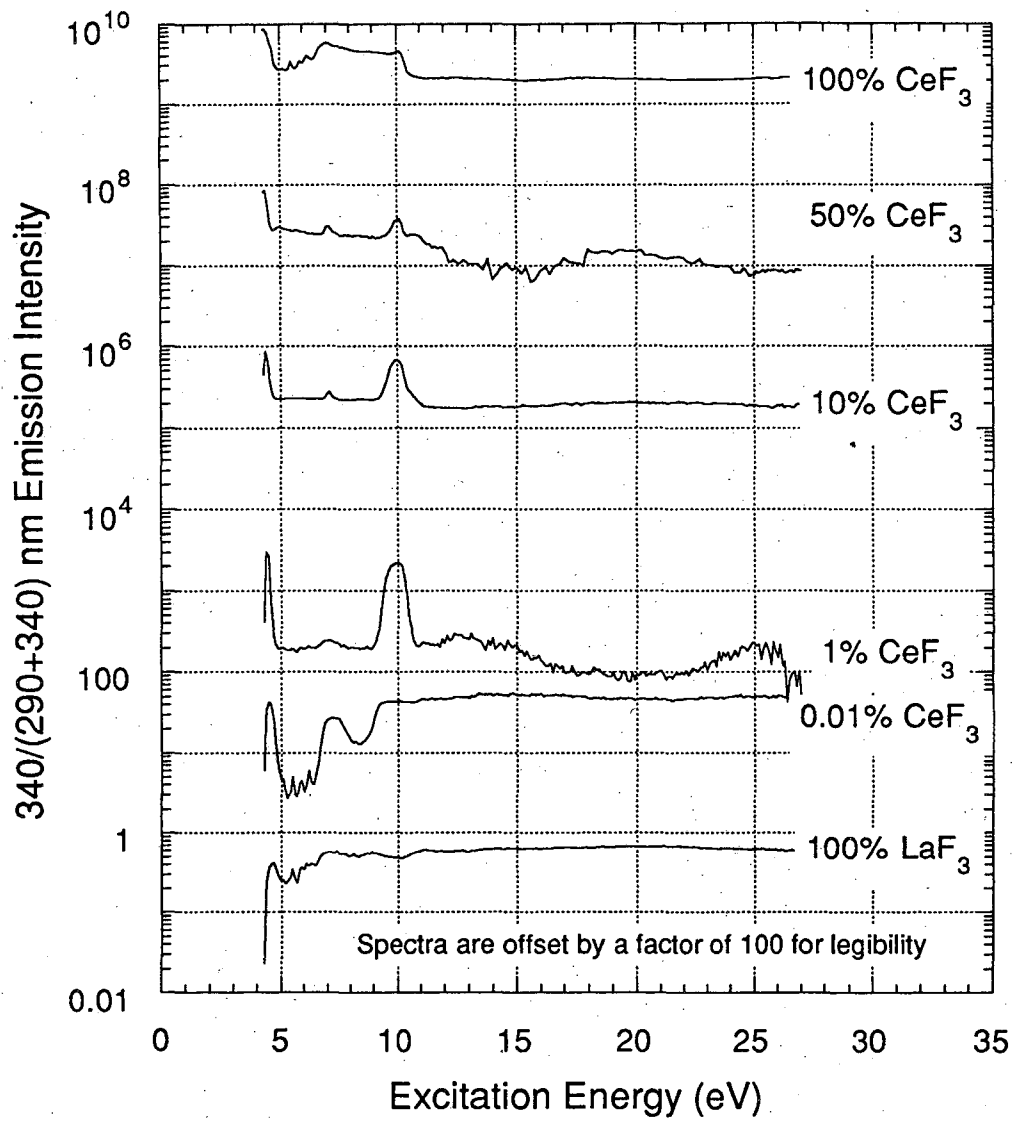


Figure 10: Ratios of fluorescence excitation spectra: 340/(290+340) nm emissions in CeF_3 , $\text{LaF}_3\text{:Ce}$ and LaF_3 .

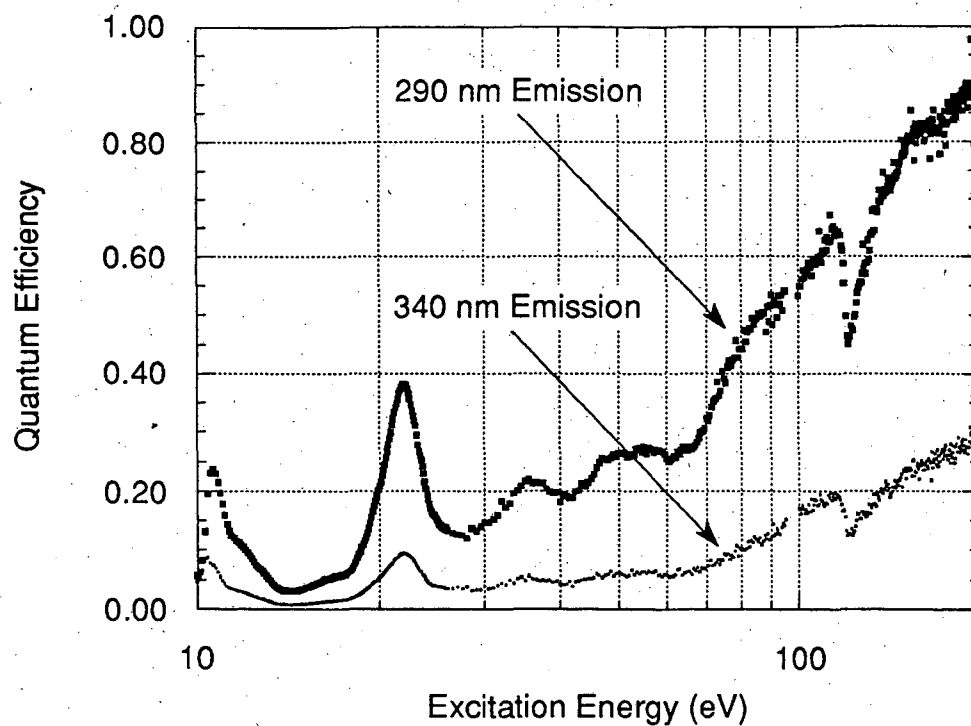


Figure 11: Quantum efficiency in CeF_3 for the 290 and 340 nm emission lines, normalized to 0.15 for the 290 nm line excited with 25 eV photons.

References

- [1] Anderson DF. Properties of the high-density scintillator cerium fluoride. *IEEE Trans. Nucl. Sci.* NS-36: pp. 137-140, 1989.
- [2] Moses WW and Derenzo SE. Cerium fluoride, a new fast, heavy scintillator. *IEEE Trans. Nucl. Sci.* NS-36: pp. 173-176, 1989.
- [3] Moses WW and Derenzo SE. The scintillation properties of cerium-doped lanthanum fluoride. *Nucl. Instr. Meth.* A299: pp. 51-56, 1990.
- [4] Anderson DF. Cerium fluoride: a scintillator for high-rate applications. *Nucl. Instr. Meth.* A287: pp. 606-612, 1990.
- [5] Ferrere D, Lebeau M, Schneegans M, et al. High resolution crystal calorimetry at LHC. *Nucl. Instr. Meth.* A315: pp. 332-336, 1992.
- [6] Lecoq P, Schussler M and Schneegans M. Progress and prospects in the development of new scintillators for future high energy physics experiments. *Nucl. Instr. Meth.* A315: pp. 337-343, 1992.
- [7] Lecoq P. Results on new scintillating crystals from the "Crystal Clear" collaboration (submitted to *IEEE Trans. Nucl. Sci.*). CERN Report No. CERN-PPE / 92-000 (pp. 1-4), November 12, 1992.
- [8] Kröger FA and Bakker J. Luminescence of cerium compounds. *Physica* 8: pp. 628-646, 1941.
- [9] Elias LR, Heaps WS and Yen WM. Excitation of uv fluorescence in LaF₃ doped with trivalent cerium and praseodymium. *Phys. Rev.* B-8: pp. 4989-4995, 1973.
- [10] Yang KH and DeLuca JA. UV fluorescence of cerium-doped lutetium and lanthanum trifluorides, potential tunable coherent sources from 2760 to 3220 Å. *App. Phys. Lett.* 31: pp. 594-596, 1977.
- [11] Pedrini C, Moine B, Gacon JC, et al. One- and two-photon spectroscopy of Ce³⁺ ions in LaF₃-CeF₃ mixed crystals. *J. Phys.: Condens. Matter* 4: pp. 5461-5470, 1992.
- [12] Wojtowicz AJ, Berman E, Koepke C, et al. Stoichiometric cerium compounds as scintillators part I: CeF₃. *IEEE Trans. Nucl. Sci.* NS-39: pp. 494-501, 1992.
- [13] Lang RJ. The spectrum of trebly ionized cerium. *Can. J. Res.* A-14: pp. 127-130, 1936.
- [14] Ehrlich DJ, Moulton PF and Osgood RM Jr. Optically pumped Ce:LaF₃ laser at 286 nm. *Opt. Lett.* 5: pp. 339-341, 1980.
- [15] Lyu LJ and Hamilton JS. Radiative and nonradiative relaxation measurements in Ce³⁺ doped crystals. *J. Lumin.* 48/49: pp. 251, 1991.
- [16] Fairley EJ and Spowart AR. Neutron scintillating glasses part III: pulse decay time measurements at room temperature. *Nucl. Instr. Meth.* 150: pp. 159-163, 1978.
- [17] Melcher CL and Schweitzer JS. Cerium-doped lutetium orthosilicate: A fast, efficient new scintillator. *IEEE Trans. Nucl. Sci.* NS-39: pp. 502-504, 1992.
- [18] Bimberg D, Robbins DJ, Wright DR, et al. CeP₅O₁₅, a new ultrafast scintillator. *Appl. Phys. Lett.* 27: pp. 67-68, 1975.
- [19] Poole RT, Jenkin JG, Liesegang J, et al. Electronic band structure of the alkali halides. I. Experimental parameters. *Phys. Rev.* B-11: pp. 5179-5196, 1975.

- [20] Kubota S, Itoh M, Ruan J, et al. Observation of interatomic radiative transition of valence electrons to outermost-core-hole states in alkali halides. *Phys. Rev. Lett.* **60**: pp. 2319-2322, 1988.
- [21] Popma TJA, van der Weg WF and Thimm K. Excitation of luminescent materials by synchrotron radiation. *J. Lumin.* **24/25**: pp. 289-292, 1981.
- [22] Berkowitz JK and Olsen JA. Investigation of luminescent materials under ultraviolet excitation energies from 5 to 25 eV. *J. Lumin.* **50**: pp. 111-121, 1991.
- [23] Sato S, Sakisaka Y and Matsukawa T. Optical absorption and photoemission spectra of rare earth (La, Ce) halides. In *Vacuum UV Radiation Physics*, pp. 414-416, (Edited by E. E. Koch, R. Maensel and C. Kunz), Pergamon Press, Braunschweig, 1975.
- [24] Dorenbos P, van Eijk CWE, Hollander RW, et al. Scintillation Properties of Nd³⁺ doped LaF₃ crystals. *IEEE Trans. Nucl. Sci.* **NS-37**: pp. 119-123, 1990.
- [25] Olson CG, Piacentini M and Lynch DW. Optical properties of single crystals of some rare-earth trifluorides, 5-34 eV. *Phys. Rev.* **B-18**: pp. 5740-5749, 1978.
- [26] Heaps WS, Elias LR and Yen WM. Vacuum-ultraviolet absorption bands of trivalent lanthanides in LaF₃. *Phys. Rev.* **B-13**: pp. 94-104, 1976.
- [27] Kim HK, Park HL, Yu I, et al. Photoluminescence studies of Ce³⁺ -doped CaS phosphor. *J. Mater. Sci. Lett.* **9**: pp. 57-58, 1990.
- [28] Cheetham AK, Fender BEF, Fuess H, et al. A powder neutron diffraction study of lanthanum and cerium trifluorides. *Acta Cryst.* **B32**: pp. 94-97, 1976.
- [29] Ilmas ER and Savikhina TI. Investigation of luminescence excitation processes in some oxygen-dominated compounds by 3 to 21 eV photons. *J. Lumin.* **1,2**: pp. 702-715, 1970.
- [30] Holl I, Lorenz E and Mageras G. A measurement of the light yield of common inorganic scintillators. *IEEE Trans. Nucl. Sci.* **NS-35**: pp. 105-109, 1988.

LAWRENCE BERKELEY LABORATORY
UNIVERSITY OF CALIFORNIA
TECHNICAL INFORMATION DEPARTMENT
BERKELEY, CALIFORNIA 94720